THE JOURNAL OF
PHYSICAL CHEMISTRY C

Article

pubs.acs.org/JPCC

Plasmon-Enhanced Triplet–Triplet Annihilation Using Silver Nanoplates

Kianoosh Poorkazem, Amelia V. Hesketh, and Timothy L. Kelly*

Department of Chemistry, University of Saskatchewan, 110 Science Place, Saskatoon, SK S7N 5C9, Canada

S Supporting Information

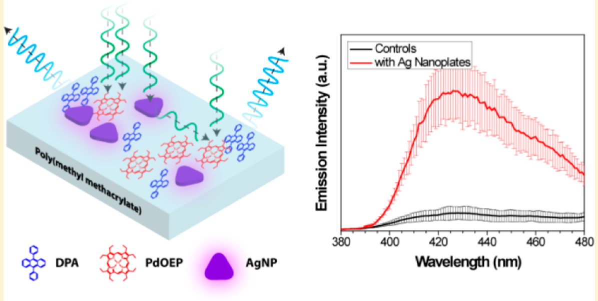

ABSTRACT: Photon upconversion processes have attracted substantial interest as a means of circumventing the Shockley–Queisser limit for single-junction photovoltaic devices. Despite this promise, the quantum yield of most upconversion processes is very low at the light intensities typical of solar radiation (~100 mW/cm^2). Additionally, bimolecular upconversion processes that rely on molecular diffusion (e.g., triplet–triplet annihilation) typically see further reductions in quantum yield when the upconverting chromophores are confined to a solid state or thin film matrix. Here we report a plasmon-based enhancement of the triplet–triplet annihilation process when silver nanoplates are embedded in poly(methyl methacrylate) thin films containing the upconverting materials palladium(II) octaethylporphyrin and 9,10-diphenylanthracene. The silver nanoplates are synthesized with localized surface plasmon resonance bands tailored to overlap strongly with the Q-band of the porphyrin, leading to enhanced light absorption within the film and higher overall triplet concentrations. Optimization of the silver nanoplate loading leads to a nearly 10-fold increase in the upconverted light intensity compared with control samples containing no silver.

■ INTRODUCTION

The Shockley–Queisser limit places a fundamental limit on the efficiency of single-junction photovoltaic devices.[1] This limit is caused by the inevitable increase in thermalization losses as the bandgap of a semiconductor is lowered, meaning that either transmission or thermalization losses can be minimized, but not both simultaneously. This restricts the power conversion efficiencies of single-junction solar cells to 31%, and devices based on crystalline Si and GaAs have already begun to approach this limit.[2] Recently, photon upconversion has been proposed as a way of circumventing the Shockley–Queisser limit; by converting two photons of low-energy light into a single photon of higher energy, photovoltaic materials with wider bandgaps can be utilized while still harvesting the low-energy portion of the solar spectrum.[3] In order to fully realize this approach, the development of highly efficient upconverting systems is required.

Upconversion processes are known to occur for a variety of small molecule dyes,[4,5] quantum dots,[6] and lanthanide compounds.[7−10] Of these, the lanthanide systems (e.g., $NaYF_4$:Yb,Er) are perhaps the most well-known; however, despite undergoing efficient photon upconversion via an energy transfer mechanism, these lanthanide phosphors suffer from narrow absorption bands in the near-infrared region due to the ionic nature of the f–f electronic transitions. This makes them highly dependent on sensitization by other chromophores[10] and limits their utility in harvesting solar radiation. In contrast, small molecule chromophores have inherently broad absorption spectra which can be readily tuned throughout the visible region by tailoring the molecular structure and through the judicious choice of functional groups. In these systems, triplet–triplet annihilation (TTA) is a well-known upconversion mechanism in which two molecules in excited triplet states combine to produce both ground state and higher-lying singlet products.[4,5] Numerous examples of TTA-based upconversion systems exist in the literature;[11−16] however, of these, the most efficient are those that utilize both a triplet sensitizer and a fluorescent emitter. The triplet sensitizer combines a high extinction coefficient with a large quantum yield for intersystem crossing, thereby producing a high concentration of excited triplet states.[17] Triplet–triplet energy transfer results in the fluorescent emitter being promoted to an excited triplet state, after which two emitter molecules undergo TTA to produce both S_0 and S_n state ($n \geq 1$) products. Assuming that the emitter has a high fluorescence quantum yield, the net result of this process is the absorption of two low-energy photons and the re-emission of one photon of higher energy. While TTA has been previously observed in thin films (as would be required in photovoltaic applications),[18−21] it is inherently a bimolecular process; as such, diffusion limitations mean that its efficiency in condensed media is often quite low.

The localized surface plasmons of noble metal nanoparticles have been shown to effectively improve the efficiency of a variety of optical and optoelectronic phenomena,[22] including

Received: December 13, 2013
Revised: February 21, 2014
Published: March 6, 2014

dx.doi.org/10.1021/jp412223m | *J. Phys. Chem. C* 2014, 118, 6398−6404

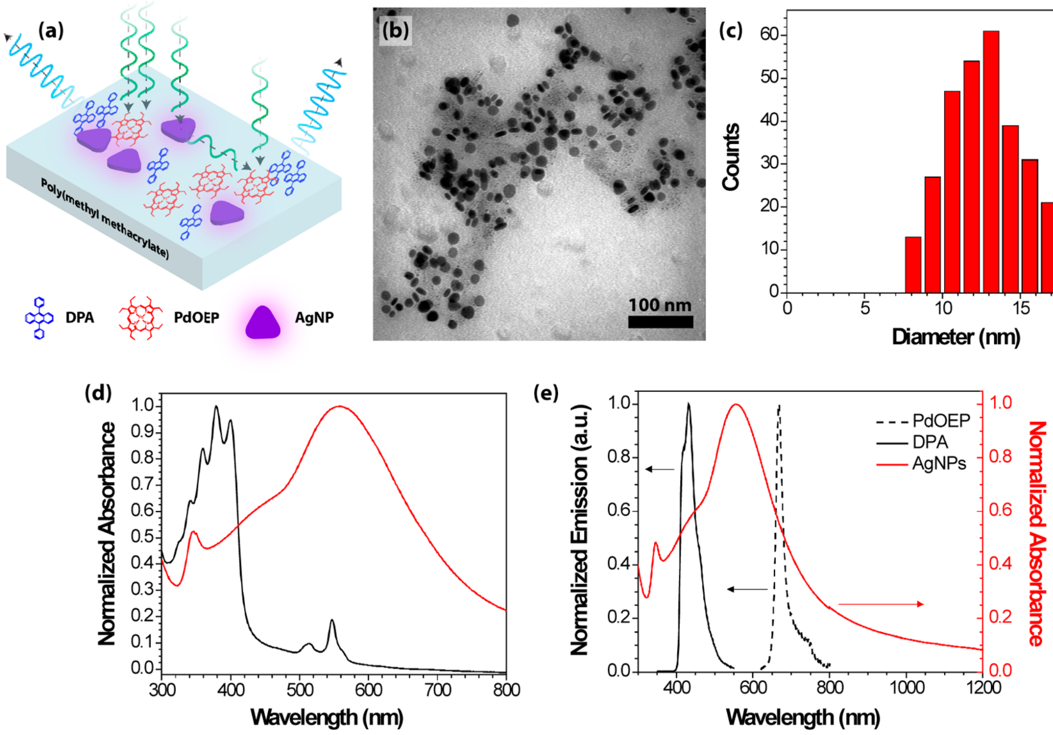

Figure 1. (a) Schematic depiction of the metal enhanced triplet−triplet annihilation process in PMMA thin films. (b) TEM image of the AgNPs after functionalization and phase transfer to chloroform. (c) AgNP particle size distribution as-determined by TEM. (d) Normalized absorption spectra of both DPA/PdOEP (black line) and the AgNPs (red line) in PMMA films. (e) Emission spectra of DPA (solid black line) and PdOEP (dashed black line) in chloroform solution when directly excited at 288 and 550 nm, respectively. The absorption spectrum of the AgNPs in chloroform solution (solid red line) is shown for comparison.

Raman scattering,[23] second harmonic generation,[24] and the performance of organic light-emitting diodes and photovoltaic devices.[25,26] One particularly important application of these plasmonic nanomaterials is metal-enhanced fluorescence (MEF).[27] This phenomenon manifests as a large increase in emission intensity when there is an overlap between the absorption or emission band of a fluorophore and the localized surface plasmon resonance (LSPR) of a metal nanoparticle in close proximity. The origins of the effect are twofold: (i) the nanoparticle can lead to increased light absorption by the fluorophore due to enhancements of the local electric field, and (ii) coupling of the fluorophore excited state to localized surface plasmons gives rise to faster emission rates and shorter excited state lifetimes. While MEF has been shown to result in enhanced emission from a wide variety of materials,[28−31] including lanthanide upconversion phosphors,[32] there are very few reports of metal-enhanced triplet−triplet annihilation. Baluschev et al. first reported a substantial increase in upconverted emission from a platinum porphyrin/polyfluorene film when it was deposited on top of a thin film of silver;[33] however, this study utilized an optical prism in a Kretschmann configuration to excite surface plasmon polariton modes in the silver film, and the necessity of the prism makes it very difficult to integrate the resultant film into most devices. Similarly, Uemura et al. were able to observe tip-enhanced upconverted emission from copper phthalocyanine films;[34] however, the necessity of the scanning tunneling microscope tip again makes this approach impractical for real-world applications. While recent studies utilizing numerical techniques have suggested that the efficiency of TTA can be dramatically improved using nanoparticle systems (e.g., silver nanocrescents),[35] there is a clear impetus to experimentally demonstrate plasmon-enhanced TTA using a simple, scalable process (e.g., nanoparticle-embedded thin films).

In this study, we report the plasmonic enhancement of triplet−triplet annihilation by the incorporation of silver nanoplates (AgNPs) into poly(methyl methacrylate) (PMMA) thin films containing palladium(II) octaethylporphyrin (PdOEP) as a triplet sensitizer and 9,10-diphenylanthracene (DPA) as a fluorescent emitter. This process is both efficient and highly scalable, producing measurable upconversion from films as thin as 40 nm and resulting in a nearly 10-fold enhancement of the upconverted emission intensity for optimized loadings of the silver nanoplates. The design of more efficient photon upconversion systems is expected to have important implications for the efficiency of a variety of optical and optoelectronic processes, most notably photovoltaic devices.

■ EXPERIMENTAL METHODS

Materials and Methods. Silver nitrate, sodium borohydride, L-ascorbic acid, trisodium citrate dihydrate, poly(sodium styrenesulfonate) ($M_w \sim 1000$ kDa), 16-mercaptohexadecanoic acid, *N*-(3-(dimethylamino)propyl)-*N*′-ethylcarbodiimide hydrochloride, dicyclohexylamine, poly(methyl methacrylate), palladium(II) octaethylporphyrin, and 9,10-diphenylanthracene were purchased from commercial suppliers (Fisher Scientific or Sigma-Aldrich) and used as received.

Transmission electron microscopy was performed on a Philips CM10 microscope operated at 80 kV. Dynamic light scattering measurements were made using a Malvern Zetasizer Nano S. Film thicknesses were measured using a D-120 Stylus profilometer from KLA Tencor. Steady state absorption spectra were acquired with a Cary 6000i UV−vis−NIR spectrophotometer. Routine emission spectra were measured using a PTI fluorometer. Photon upconversion measurements were made using a 532 nm CW laser excitation source and a custom-modified SPEX fluorometer. The detector was placed at a 45° angle relative to the excitation source in order to eliminate reflected light, and a 532 nm notch filter was used to further prevent any scattered laser light from reaching the detector. A 10-step calibrated neutral density filter was used to control the excitation power density.

Synthesis of Silver Nanoplates. The AgNPs were synthesized according to literature procedures.[36] Silver seed particles were prepared by combining aqueous trisodium citrate (5 mL, 2.5 mM), aqueous poly(sodium styrenesulfonate) (0.25 mL, 500 mg L^{-1}), and aqueous sodium borohydride (0.3 mL, 10 mM), followed by the addition of aqueous $AgNO_3$ (5 mL, 0.5 mM) at a rate of 2 mL min^{-1}. The silver nanoplates were then synthesized by combining 50 mL of deionized water, 750 μL of 10 mM aqueous ascorbic acid, and 9−10 mL of silver seed solution (the exact amount required to produce nanoplates with $\lambda_{LSPR} \sim 560$ nm varied slightly with each preparation), followed by the addition of aqueous $AgNO_3$ (30 mL, 0.5 mM) at a rate of 1 mL min^{-1}. Additional trisodium citrate solution (5 mL, 25 mM) was then added to further stabilize the AgNPs.

Phase Transfer of Silver Nanoplates. The AgNPs were functionalized and transferred to chloroform following a literature procedure.[37] A solution of 16-mercaptohexadecanoic acid (1.17 mL, 5 mM in ethanol) was added to 96 mL of the as-prepared silver nanoprism solution, and the mixture was stirred for 20 min. The product was centrifuged for 2 h at 13 000 rpm. The supernatant was discarded, and the thiol-functionalized AgNPs were resuspended in ethanol to a final volume of 4 mL. A portion of the resulting solution (1 mL) was added dropwise to 10 mL of an ethanolic solution composed of 50 mM *N*-(3-(dimethylamino)propyl)-*N*′-ethylcarbodiimide hydrochloride and 50 mM dicyclohexylamine. After 15 min, the functionalized silver nanoplates precipitated and were isolated by centrifugation at 13 000 rpm for 1 h. The supernatant was decanted, and the precipitate, once dry, was resuspended in chloroform.

Film Preparation. Glass slides are precleaned by sonicating sequentially in detergent, distilled water, and ethanol, followed by a UV-ozone treatment (15 min). Chloroform solutions containing PMMA, PdOEP, and DPA at concentrations of 2.1 mg/mL, 0.15 mM, and 5.1 mM and varying amounts of the AgNP stock solution were prepared. Films were prepared by spin-coating at 3000 rpm for 20 s followed by 100 rpm for 5 s. All solutions and samples were kept in the dark when not in use.

■ RESULTS AND DISCUSSION

Synthesis and Phase Transfer of Silver Nanoplates. In thin films of even the most highly absorbing materials, a substantial portion of the incident light is lost due to transmission. In order to minimize these losses in the PdOEP/DPA/PMMA system, silver nanoplates were synthesized using a highly tunable process,[36] such that their in-plane dipole LSPR band overlapped strongly with the Q-band of the PdOEP (Figure 1). In the first step of the nanoplate synthesis, small silver nanoparticles were synthesized as seed particles. The nanoseeds were subsequently grown into platelike nanoparticles via the addition of $AgNO_3$ in the presence of ascorbic acid.[36] Based on the relative ratio of seed particles to $AgNO_3$, the nanoparticles can be grown into nanoplates with varying aspect ratios; since the aspect ratio of the nanoparticle controls the frequency of its localized surface plasmons, this process enables the synthesis of AgNPs with highly tunable LSPR bands. In order to maximize plasmonic effects throughout the entire thickness of the PMMA film, we have adopted the approach of directly embedding the AgNPs into the polymer matrix, rather than confining them to either the substrate/polymer or polymer/air interfaces. This requires that the AgNPs be codissolved in a common solvent along with the PdOEP, DPA, and PMMA. This was accomplished by first functionalizing the surface of the AgNPs with 16-mercaptohexadecanoic acid. The terminal carboxylate of the thiol ligand provides a functional group that can be readily modified with hydrophobic headgroups. Following an established phase transfer protocol,[37] the 16-mercaptohexadecanoic acid-derivatized nanoplates were reacted with dicyclohexylamine and a carbodiimide coupling agent to produce a hydrophobic nanoparticle surface. The AgNPs were then isolated by centrifugation and were readily redispersed in chloroform.

Figure 1b shows a TEM image of the silver nanoparticles after undergoing the phase transfer process. As can be seen from the image, the particles are platelike in structure and range from round to pseudotriangular in shape. The anisotropic particle shape plays two important roles in the present study. First, it red-shifts the position of the LSPR band well into the visible region (Figure S1a), which is not feasible with spherical silver nanoparticles.[38] Second, anisotropic nanoparticles have been shown to produce larger near-field enhancements when compared to their spherical analogues;[22,38] as such, silver nanoplates and nanoprisms have found extensive use in a variety of plasmonic applications.[22,39,40] The size distribution of the AgNPs is shown in Figure 1c. The average diameter of the nanoplates was determined to be 13 ± 2 nm, which is noticeably smaller than the average diameter determined by dynamic light scattering (Figure S1b). The dicyclohexylamide-terminated nanoparticles are known to exist as stable aggregates in chloroform solution,[37] and it is these aggregates that are reflected in the light scattering data. This may give rise to several important effects, including the formation of "hot spots" within the polymer film, where multiple nanoparticles in close proximity produce coupled plasmon modes and strongly increased near-field enhancements. Previous work has shown that the aggregation state of the metal nanoparticle can dramatically affect the relative degree of MEF (as compared to fluorescence quenching), with aggregated nanoparticles giving rise to higher emission quantum yields.[41] As such, the morphology of the AgNPs used in the current study suggests that they may be of great utility in MEF applications.

Figure 1 illustrates the overall strategy used in this work. When excited by light resonant with the LSPR mode, the AgNPs create substantial near-field enhancements within the thin film, leading to increased levels of light absorption by the PdOEP. This should in turn lead to an increased local concentration of excited triplet states (of both sensitizer and emitter) within the film, and a corresponding increase in both phosphorescence and upconverted emission intensities. Alternatively, resonant scattering from the AgNPs could also lead to an increase in light absorption by the sensitizer. Since the oscillating dipole of a localized surface plasmon is an excellent emitter of electromagnetic radiation, larger metal nanoparticles become highly efficient scatterers of light when the frequency is resonant with the LSPR band. As such, by angularly dispersing the incident light, the AgNPs may serve to increase the effective optical path length of the film, thereby leading to increased levels of light absorption and TTA. However, in order for either of these upconversion mechanisms to be active, a primary requirement is that there has to be substantial overlap between the absorption spectrum of the triplet sensitizer and the LSPR band of the metal nanoparticle. The absorption spectra of both PdOEP/DPA/PMMA and AgNP/PMMA films are shown in Figure 1d. When embedded in the PMMA matrix, the AgNPs have a broad in-plane dipole LSPR band[38] centered at 560 nm. Given the breadth of this peak, it overlaps very well with both the Q-bands of the PdOEP (centered at 512 and 546 nm) and the wavelength of the laser excitation source used in this study (532 nm). As such, the AgNPs are expected to give rise to substantial near-field enhancements at the wavelengths relevant to this work. Radiative decay engineering (coupling of the emitter excited state to the LSPR) is also known to give rise to increased luminescence intensities; however, this mechanism requires overlap between the LSPR and the *emission* band of the luminophore. Very poor overlap is observed between the AgNP LSPR band and both the DPA fluorescence and PdOEP phosphorescence bands (Figure 1e), and we would therefore expect any observed increases in upconverted emission to be due to an increase in light absorption by the PdOEP.

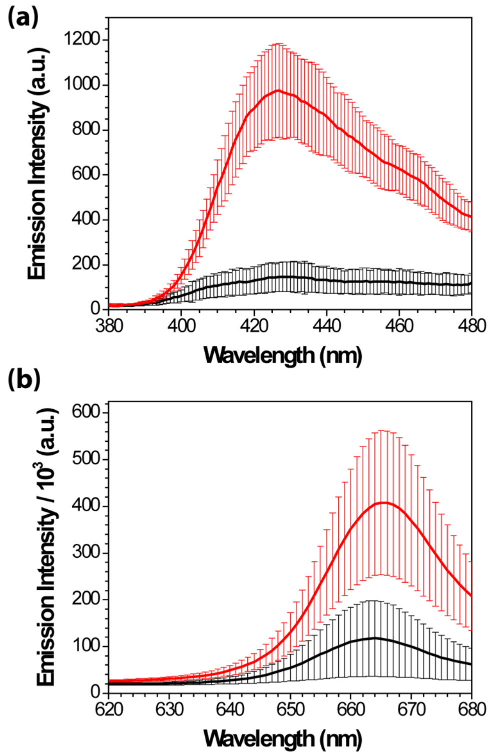

Figure 2. Emission spectra of the control (black lines) and AgNP-containing (red lines) DPA/PdOEP/PMMA films showing both (a) DPA fluorescence as a result of TTA and (b) PdOEP phosphorescence. Spectra are the average of either 20 (for DPA fluorescence of the control samples) or 6 (all other spectra) separate films. The error bars correspond to plus or minus one standard deviation from the mean.

Photon Upconversion Measurements. In order to study metal-enhanced TTA in the solid state, both PdOEP/DPA/PMMA and PdOEP/DPA/AgNP/PMMA solutions were prepared in chloroform, and thin films of the materials were spin-coated onto precleaned glass slides. Both solutions maintained equal concentrations of the PdOEP, DPA, and PMMA, with the only variable being either the presence or absence of the silver nanoplates. Profilometry measurements indicated an average film thickness of 30 ± 20 and 40 ± 20 nm for the films with and without AgNPs, respectively. The samples were mounted in a custom-made sample holder such that the PMMA films were held under vacuum during the measurements (Figure S2). This eliminates the diffusion of oxygen into the films, which would otherwise be expected to efficiently quench the PdOEP T_1 states. Figure 2 shows both the Stokes and anti-Stokes shifted emission for the thin films when excited with a 532 nm CW laser. In order to ensure the reproducibility of the results, and to eliminate the effects of any variations in film thickness or homogeneity, 6 separate PdOEP/DPA/AgNP/PMMA films and 20 separate PdOEP/DPA/PMMA control samples were measured, and the spectra were averaged. The emission data in the region of 600−680 nm (Figure 2b) reveal an approximately 3.5-fold increase in the PdOEP phosphorescence intensity upon inclusion of the silver nanoplates into the film. This result is entirely consistent with an increase in the absorption cross-section of the PdOEP chromophore when placed in the AgNP near-field. On the basis of this increase in the PdOEP triplet concentration, one would further expect that the intensity of upconverted emission would also be enhanced. Figure 2a shows the anti-Stokes shifted emission that occurs as a result of the TTA process. Again, a clear increase in emission intensity is observed for the films containing the AgNPs; however, in this case, the difference is much more pronounced, with the upconverted emission intensity from the AgNP-containing films a factor of 6.6 times higher than that of the PdOEP/DPA/PMMA control samples. This yields an approximately 2:1 ratio for the plasmonic enhancement of TTA and phosphorescence. Since TTA is inherently bimolecular in the concentration of PdOEP T_1 states, it is expected to have a nonlinear response to the number of absorbed photons,[42] whereas the PdOEP phosphorescence is inherently linear in absorbed photon flux. As such, the upconverted emission intensity is much more sensitive to the absorption cross section of the triplet sensitizer than the phosphorescence intensity. Therefore, the observed 2:1 ratio of enhancement in TTA/phosphorescence is entirely consistent with an increase in the PdOEP absorption cross section. However, as discussed previously, one other possibility is that these changes are due to increased emission rates in both the DPA and PdOEP.[27] If this were the case, the shorter PdOEP excited state lifetime would be expected to rapidly deplete the reservoir of excited triplets, in turn leading to a net reduction in the TTA efficiency. Since this is not observed, and given that neither the DPA nor the PdOEP emission band overlaps significantly with the LSPR of the AgNPs (Figure 1e), this is considered unlikely. In order to further prove that an increase in the emission rate is not responsible for the observed increase in emission intensity, both DPA/PMMA and DPA/AgNP/PMMA films were prepared. Addition of the AgNPs results in no measurable increase in fluorescence intensity upon direct excitation of the DPA (λ_{exc} = 350 nm) (Figure S3), suggesting that the intensity increases observed in Figure 2 arise solely from an increase in the PdOEP absorption cross section.

Power Dependency Measurements. The extinction coefficient of the Q-band for most Pd porphyrins is low, and therefore excitation into the Q-band typically results in a low density of triplet states and a low TTA efficiency. As a result, triplet decay is primarily unimolecular in nature, leading to a quadratic dependence of TTA on excitation power (especially at low excitation intensities).[42] If the concentration of excited-state triplets is increased (either by increasing the extinction coefficient at the excitation wavelength or by increasing the excitation power), bimolecular triplet decay (i.e., TTA) becomes favored, leading to a more linear dependence on excitation power. The development of new triplet sensitizers, such as Ir,[43] Pt,[44] and Ru[45] complexes, and organic molecules such as C_{60}[17] and various BODIPY dyes,[46,47] has been shown to lead to more linear power dependencies in the TTA process. In this work, the plasmon-based increase of the PdOEP absorption cross section is used in a similar way.

In order to further probe the dependency of the TTA process on the PdOEP triplet concentration, power dependency measurements were carried out on two separate films for both control and AgNP-containing samples. Six separate combinations of neutral density filters were used to attenuate the 532 nm excitation source over a range of power densities. Figure 3 shows the results of these measurements. The intensity of DPA fluorescence is plotted against the intensity of PdOEP phosphorescence in a double-logarithmic plot. Since the PdOEP phosphorescence is directly related to the overall yield of T_1 states, the PdOEP phosphorescence intensity is a convenient surrogate for the total number of photons absorbed by the porphyrin. Additionally, by plotting the upconverted emission against the phosphorescence intensity (rather than the incident power density), the data are automatically corrected for any photobleaching or two-photon absorption that may occur at the high power densities used.

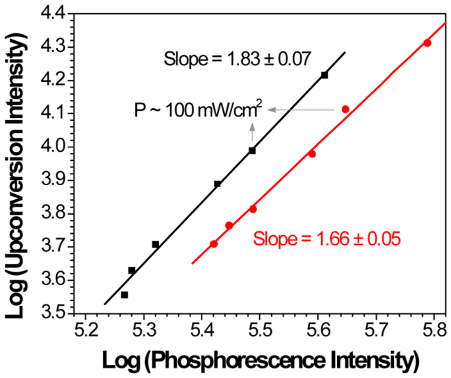

Figure 3. Power dependency measurements obtained for both the control (black squares) and AgNP-containing (red circles) films. The data are the average of two separate films. The six data points in each data set correspond to six different power densities, which increase from left to right. The data points corresponding to ~1 sun intensity (100 mW/cm^2) are labeled. Upconverted and phosphorescence peak intensities were measured at 430 and 662 nm, respectively.

As can be seen in Figure 3, the line of best fit for the DPA/PdOEP/PMMA control samples has a slope of 1.83 ± 0.07, indicative of a roughly quadratic dependence of the TTA process on the number of T_1 states. This is consistent with predominantly pseudo-first-order decay of the sensitizer/annihilator triplets, typical of low-power regimes.[42] In contrast, the line of best fit for the samples containing AgNPs has a slope of 1.66 ± 0.05. This lower slope suggests that a greater proportion of the triplets are decaying via bimolecular processes than in the case of the control samples. This implies a higher triplet concentration within the AgNP-containing film (as would typically be observed at higher power densities) and is entirely consistent with plasmonic near-field effects producing an increased level of light absorption within the film (i.e., effectively increasing the local power density). This results in an intermediate power dependency that falls midway between the linear and quadratic regimes.

Importantly, the data also reveal that both the phosphorescence and upconversion emission intensities are higher for the AgNP-containing samples than the controls at a given power density. This is seen as an offset (both horizontal and vertical) between the two power density plots in Figure 3 and further reinforces the effectiveness of both the metal enhanced phosphorescence and metal enhanced TTA processes.

Optimization of Silver Nanoplate Loading. In order to optimize the silver nanoplate loading, the concentration of the silver nanoplates in the DPA/PdOEP/AgNP/PMMA stock solutions was systematically varied. Owing to the difficulties involved in quantifying the AgNP concentration after several synthesis and phase transfer steps, a common AgNP stock solution with an optical density of 0.81 (as measured at the λ_{LSPR} in chloroform solution using a 1 mm path length cuvette) was employed. Varying amounts of this stock solution were blended with aliquots of a common DPA/PdOEP/PMMA stock solution and diluted with chloroform to the same final volume, producing solutions that were 0% (control samples), 5%, 10%, 20%, and 30% AgNP stock solution by volume. Thin films were again prepared by spin-coating, and their emissive properties were evaluated using a 532 nm CW laser excitation source. Figures S4 and S5 show the averaged emission spectra for each set of samples in the DPA fluorescence and PdOEP phosphorescence spectral ranges, respectively. Figure 4 shows the peak intensity (measured at 430 nm for DPA fluorescence and 662 nm for PdOEP phosphorescence) as a function of the silver nanoplate loading. At very low AgNP concentrations (5–10%) there is very little change in the emissive properties of the films, but there is a substantial increase in both emission intensities as the AgNP concentration is increased to 20%. After this point, the emission intensities begin to level off, likely

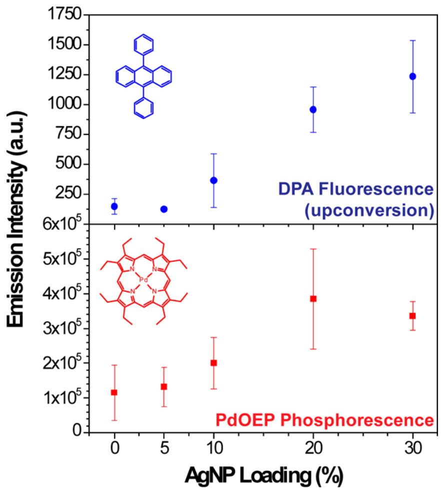

Figure 4. Emission intensity of DPA fluorescence resulting from TTA (top, blue circles) and PdOEP phosphorescence (bottom, red squares) as a function of AgNP loading. The error bars represent plus or minus one standard deviation from the mean. Upconverted and phosphorescence peak intensities were measured at 430 and 662 nm, respectively.

because of competitive quenching effects as the concentration of Ag within the film is increased. For the optimized AgNP concentration of 30%, however, we were able to realize an 8.5-fold increase in the DPA fluorescent emission, indicating that the efficiency of the TTA process increased by nearly an order of magnitude.

In order to validate our results, we carried out a series of statistical tests on the data, including both ANOVA and pairwise *t* tests at the 95% confidence level. The results of these tests are shown in Tables S1–S3. The ANOVA test clearly reveals a dependence of both the phosphorescence emission intensity and upconverted emission intensity on the silver nanoplate loading. The *t* tests further reveal that there is no statistically significant change in either DPA fluorescence or PdOEP phosphorescence upon increasing the AgNP concentration to either 5% or 10%; however, upon increasing the concentration to 20%, the change becomes significant for both the upconverted emission and phosphorescence. Profilometry measurements were again carried out on all films to ensure that the observed differences were not due to differences in film thickness (Figure S6). Power dependency measurements were also carried out on representative films (Figure S7), with the slopes of the double-logarithmic plots all lying in the range of 1.7–2.0, as expected.

■ CONCLUSIONS

We have successfully used the plasmonic effects of anisotropic silver nanoplates to realize substantial increases in the efficiency of the triplet–triplet annihilation process. The increase in upconverted emission is attributed to an increase in the local density of excited triplets, owing to an increased absorption cross-section of the PdOEP sensitizer in the presence of the AgNP near-field. The 8.5-fold increase in upconverted emission intensity is extremely promising, and it is expected that with further modifications to the nanoparticle size and shape, as well as the mechanical properties of the polymer,[20] this increase may be further improved. These results suggest that TTA may soon become a viable method of photon upconversion in thin film devices, even at the relatively low power densities typical of unconcentrated solar radiation. This has important implications for the efficiency of photovoltaic devices, in particular for the Shockley–Queisser efficiency limit.

■ ASSOCIATED CONTENT

Ⓢ Supporting Information

UV–vis spectra, dynamic light scattering measurements, schematic of the sample holder, emission spectra, results of statistical tests, profilometry data, and power dependency measurements. This material is available free of charge via the Internet at http://pubs.acs.org.

■ AUTHOR INFORMATION

Corresponding Author

*E-mail tim.kelly@usask.ca; Tel +1-306-966-4666 (T.L.K.).

Notes

The authors declare no competing financial interest.

■ ACKNOWLEDGMENTS

The Natural Sciences and Engineering Research Council of Canada (NSERC) and the University of Saskatchewan are acknowledged for financial support. T.L.K. is a Canada Research Chair in Photovoltaics. The research was undertaken, in part, thanks to funding from the Canada Research Chair program. A.V.H. thanks the Inorganic Chemistry Exchange (ICE) program and NSERC for an Undergraduate Student Research Award (USRA). Prof. Ronald Steer is acknowledged for helpful discussions.

■ REFERENCES

(1) Shockley, W.; Queisser, H. J. Detailed Balance Limit of Efficiency of p-n Junction Solar Cells. *J. Appl. Phys.* **1961**, *32*, 510–519.

(2) Green, M. A.; Emery, K.; Hishikawa, Y.; Warta, W.; Dunlop, E. D. Solar Cell Efficiency Tables (Version 41). *Prog. Photovolt. Res. Appl.* **2013**, *21*, 1–11.

(3) Huang, X.; Han, S.; Huang, W.; Liu, X. Enhancing Solar Cell Efficiency: the Search for Luminescent Materials as Spectral Converters. *Chem. Soc. Rev.* **2013**, *42*, 173–201.

(4) Zhao, J.; Ji, S.; Guo, H. Triplet-Triplet Annihilation Based Upconversion: from Triplet Sensitizers and Triplet Acceptors to Upconversion Quantum Yields. *RSC Adv.* **2011**, *1*, 937–950.

(5) Singh-Rachford, T. N.; Castellano, F. N. Photon Upconversion Based on Sensitized Triplet–Triplet Annihilation. *Coord. Chem. Rev.* **2010**, *254*, 2560–2573.

(6) Deutsch, Z.; Neeman, L.; Oron, D. Luminescence Upconversion in Colloidal Double Quantum Dots. *Nat. Nanotechnol.* **2013**, *8*, 649–653.

(7) Boyer, J.-C.; Cuccia, L. A.; Capobianco, J. A. Synthesis of Colloidal Upconverting $NaYF_4$: Er^{3+}/Yb^{3+} and Tm^{3+}/Yb^{3+} Monodisperse Nanocrystals. *Nano Lett.* **2007**, *7*, 847–852.

(8) Wang, F.; Han, Y.; Lim, C. S.; Lu, Y.; Wang, J.; Xu, J.; Chen, H.; Zhang, C.; Hong, M.; Liu, X. Simultaneous Phase and Size Control of Upconversion Nanocrystals Through Lanthanide Doping. *Nature* **2010**, *463*, 1061–1065.

(9) Wang, F.; Liu, X. Recent Advances in the Chemistry of Lanthanide-Doped Upconversion Nanocrystals. *Chem. Soc. Rev.* **2009**, *38*, 976–989.

(10) Zou, W.; Visser, C.; Maduro, J. A.; Pshenichnikov, M. S.; Hummelen, J. C. Broadband Dye-Sensitized Upconversion of Near-Infrared Light. *Nat. Photonics* **2012**, *6*, 560–564.

(11) Islangulov, R. R.; Kozlov, D. V.; Castellano, F. N. Low Power Upconversion using MLCT Sensitizers. *Chem. Commun.* **2005**, 3776–3778.

(12) Baluschev, S.; Yakutkin, V.; Miteva, T.; Avlasevich, Y.; Chernov, S.; Aleshchenkov, S.; Nelles, G.; Cheprakov, A.; Yasuda, A.; Müllen, K.; Wegner, G. Blue-Green Up-Conversion: Noncoherent Excitation by NIR Light. *Angew. Chem., Int. Ed.* **2007**, *46*, 7693–7696.

(13) Baluschev, S.; Jacob, J.; Avlasevich, Y. S.; Keivanidis, P. E.; Miteva, T.; Yasuda, A.; Nelles, G.; Grimsdale, A. C.; Müllen, K.; Wegner, G. Enhanced Operational Stability of the Up-Conversion Fluorescence in Films of Palladium–Porphyrin End-Capped Poly(pentaphenylene). *ChemPhysChem* **2005**, *6*, 1250–1253.

(14) Sugunan, S. K.; Greenwald, C.; Paige, M. F.; Steer, R. P. Efficiency of Noncoherent Photon Upconversion by Triplet–Triplet Annihilation: The C_{60} Plus Anthanthrene System and the Importance of Tuning the Triplet Energies. *J. Phys. Chem. A* **2013**, *117*, 5419–5427.

(15) Keivanidis, P. E.; Baluschev, S.; Miteva, T.; Nelles, G.; Scherf, U.; Yasuda, A.; Wegner, G. Up-Conversion Photoluminescence in Polyfluorene Doped with Metal(II)–Octaethyl Porphyrins. *Adv. Mater.* **2003**, *15*, 2095–2098.

(16) Du, P.; Eisenberg, R. Energy Upconversion Sensitized by a Platinum(II) Terpyridyl Acetylide Complex. *Chem. Sci.* **2010**, *1*, 502–506.

(17) Zhao, J.; Wu, W.; Sun, J.; Guo, S. Triplet Photosensitizers: from Molecular Design to Applications. *Chem. Soc. Rev.* **2013**, *42*, 5323–5351.

(18) Simon, Y. C.; Weder, C. Low-Power Photon Upconversion Through Triplet-Triplet Annihilation in Polymers. *J. Mater. Chem.* **2012**, *22*, 20817–20830.

(19) Islangulov, R. R.; Lott, J.; Weder, C.; Castellano, F. N. Noncoherent Low-Power Upconversion in Solid Polymer Films. *J. Am. Chem. Soc.* **2007**, *129*, 12652−12653.

(20) Singh-Rachford, T. N.; Lott, J.; Weder, C.; Castellano, F. N. Influence of Temperature on Low-Power Upconversion in Rubbery Polymer Blends. *J. Am. Chem. Soc.* **2009**, *131*, 12007−12014.

(21) O'Brien, J. A.; Rallabandi, S.; Tripathy, U.; Paige, M. F.; Steer, R. P. Efficient S2 State Production in ZnTPP−PMMA Thin Films by Triplet−Triplet Annihilation: Evidence of Solute Aggregation in Photon Upconversion Systems. *Chem. Phys. Lett.* **2009**, *475*, 220−222.

(22) Schuller, J. A.; Barnard, E. S.; Cai, W.; Jun, Y. C.; White, J. S.; Brongersma, M. L. Plasmonics for Extreme Light Concentration and Manipulation. *Nat. Mater.* **2010**, *9*, 193−204.

(23) Cao, Y. C.; Jin, R.; Mirkin, C. A. Nanoparticles with Raman Spectroscopic Fingerprints for DNA and RNA Detection. *Science* **2002**, *297*, 1536−1540.

(24) Bouhelier, A.; Beversluis, M.; Hartschuh, A.; Novotny, L. Near-Field Second-Harmonic Generation Induced by Local Field Enhancement. *Phys. Rev. Lett.* **2003**, *90*, 013903.

(25) Ozbay, E. Plasmonics: Merging Photonics and Electronics at Nanoscale Dimensions. *Science* **2006**, *311*, 189−193.

(26) Atwater, H. A.; Polman, A. Plasmonics for Improved Photovoltaic Devices. *Nat. Mater.* **2010**, *9*, 205−213.

(27) Geddes, C. D. *Metal Enhanced Fluorescence*; John Wiley & Sons, Inc.: Hoboken, NJ, 2010.

(28) Zhang, Y.; Aslan, K.; Previte, M. J. R.; Geddes, C. D. Metal-Enhanced S2 Fluorescence from Azulene. *Chem. Phys. Lett.* **2006**, *432*, 528−532.

(29) Previte, M. J. R.; Aslan, K.; Zhang, Y.; Geddes, C. D. Metal-Enhanced Surface Plasmon-Coupled Phosphorescence. *J. Phys. Chem. C* **2007**, *111*, 6051−6059.

(30) Aslan, K.; Holley, P.; Geddes, C. D. Metal-Enhanced Fluorescence from Silver Nanoparticle-Deposited Polycarbonate Substrates. *J. Mater. Chem.* **2006**, *16*, 2846−2852.

(31) Aslan, K.; Wu, M.; Lakowicz, J. R.; Geddes, C. D. Fluorescent Core−Shell Ag@SiO$_2$ Nanocomposites for Metal-Enhanced Fluorescence and Single Nanoparticle Sensing Platforms. *J. Am. Chem. Soc.* **2007**, *129*, 1524−1525.

(32) Zhang, W.; Ding, F.; Chou, S. Y. Large Enhancement of Upconversion Luminescence of NaYF$_4$:Yb^{3+}/Er^{3+} Nanocrystal by 3D Plasmonic Nano-Antennas. *Adv. Mater.* **2012**, *24*, OP236−OP241.

(33) Baluschev, S.; Yu, F.; Miteva, T.; Ahl, S.; Yasuda, A.; Nelles, G.; Knoll, W.; Wegner, G. Metal-Enhanced Up-Conversion Fluorescence: Effective Triplet−Triplet Annihilation near Silver Surface. *Nano Lett.* **2005**, *5*, 2482−2484.

(34) Uemura, T.; Furumoto, M.; Nakano, T.; Akai-Kasaya, M.; Saito, A.; Aono, M.; Kuwahara, Y. Local-Plasmon-Enhanced Up-conversion Fluorescence from Copper Phthalocyanine. *Chem. Phys. Lett.* **2007**, *448*, 232−236.

(35) Ashwin, C. A.; Aitzol, G.-E.; Hadiseh, A.; Jennifer, A. D. Toward High-Efficiency Solar Upconversion with Plasmonic Nanostructures. *J. Opt.* **2012**, *14*, 024008.

(36) Aherne, D.; Ledwith, D. M.; Gara, M.; Kelly, J. M. Optical Properties and Growth Aspects of Silver Nanoprisms Produced by a Highly Reproducible and Rapid Synthesis at Room Temperature. *Adv. Funct. Mater.* **2008**, *18*, 2005−2016.

(37) Liu, L.; Kelly, T. L. Phase Transfer of Triangular Silver Nanoprisms from Aqueous to Organic Solvent by an Amide Coupling Reaction. *Langmuir* **2013**, *29*, 7052−7060.

(38) Kelly, K. L.; Coronado, E.; Zhao, L. L.; Schatz, G. C. The Optical Properties of Metal Nanoparticles: the Influence of Size, Shape, and Dielectric Environment. *J. Phys. Chem. B* **2003**, *107*, 668−677.

(39) Chen, Y.; Munechika, K.; Ginger, D. S. Dependence of Fluorescence Intensity on the Spectral Overlap between Fluorophores and Plasmon Resonant Single Silver Nanoparticles. *Nano Lett.* **2007**, *7*, 690−696.

(40) Kulkarni, A. P.; Noone, K. M.; Munechika, K.; Guyer, S. R.; Ginger, D. S. Plasmon-Enhanced Charge Carrier Generation in Organic Photovoltaic Film Using Silver Nanoprisms. *Nano Lett.* **2010**, *10*, 1501−1505.

(41) Ostrowski, J. C.; Mikhailovsky, A.; Bussian, D. A.; Summers, M. A.; Buratto, S. K.; Bazan, G. C. Enhancement of Phosphorescence by Surface-Plasmon Resonances in Colloidal Metal Nanoparticles: The Role of Aggregates. *Adv. Funct. Mater.* **2006**, *16*, 1221−1227.

(42) Haefele, A.; Blumhoff, J.; Khnayzer, R. S.; Castellano, F. N. Getting to the (Square) Root of the Problem: How to Make Noncoherent Pumped Upconversion Linear. *J. Phys. Chem. Lett.* **2012**, *3*, 299−303.

(43) Ma, L.; Guo, H.; Li, Q.; Guo, S.; Zhao, J. Visible Light-Harvesting Cyclometalated Ir(III) Complexes as Triplet Photosensitizers for Triplet-Triplet Annihilation Based Upconversion. *Dalton Trans.* **2012**, *41*, 10680−10689.

(44) Kwong, R. C.; Sibley, S.; Dubovoy, T.; Baldo, M.; Forrest, S. R.; Thompson, M. E. Efficient, Saturated Red Organic Light Emitting Devices Based on Phosphorescent Platinum(II) Porphyrins. *Chem. Mater.* **1999**, *11*, 3709−3713.

(45) Wu, W. H.; Sun, J. F.; Cui, X. N.; Zhao, J. Z. Observation of the Room Temperature Phosphorescence of Bodipy in Visible Light-Harvesting Ru(II) Polyimine Complexes and Application as Triplet Photosensitizers for Triplet-Triplet-Annihilation Upconversion and Photocatalytic Oxidation. *J. Mater. Chem. C* **2013**, *1*, 4577−4589.

(46) Chen, Y.; Zhao, J.; Xie, L.; Guo, H.; Li, Q. Thienyl-Substituted BODIPYs with Strong Visible Light-Absorption and Long-Lived Triplet Excited States as Organic Triplet Sensitizers for Triplet-Triplet Annihilation Upconversion. *RSC Adv.* **2012**, *2*, 3942−3953.

(47) Wu, W. H.; Guo, H. M.; Wu, W. T.; Ji, S. M.; Zhao, J. Z. Organic Triplet Sensitizer Library Derived from a Single Chromophore (BODIPY) with Long-Lived Triplet Excited State for Triplet-Triplet Annihilation Based Upconversion. *J. Org. Chem.* **2011**, *76*, 7056−7064.